Electronic Supplementary Material (ESI) for Energy & Environmental Science.

Rectifying Interphase for Preventing Li Dendrite Propagation in Solid-State Electrolytes

Xuhui Yao,[#a,b] Xuekun Lu,[#c,d] Yundong Zhou,[b] Tomáš Šamořil,[e] Jinxin Bi,[a] Mateus G. Masteghin,[a] Huixing Zhang,[b] Leslie Askew,[a] JeongWon Kim,[f] Fangyu Xiong,[g] Jianan Wang,[h] David C. Cox,[a] Tan Sui,[b,i] Ian Gilmore,[b] S. Ravi P. Silva,[a] Liqiang Mai,[g] Gareth Hinds,[b] Paul R. Shearing,*[c] Juyeon Park,*[b] Yunlong Zhao*[a,b]

Experimental Section

Sputtering deposition for on-chip devices and LLZTO-RI pellets

The on-chip devices were prepared by a direct current sputter deposition technique (MPS 500 System, JLS Designs Ltd) on a Si wafer with a 200 nm SiO_2 coating layer. The deposition process was conducted under pressure below 10^{-6} Pa, direct current power of 150 W, and an Ar rate of 20 sccm. Al metal, Ti metal and p-Si targets were used to deposit corresponding layers. For the TiO_2 deposition, a Ti metal target was used, and extra O_2 gas with a rate of 1.2 sccm was pumped into the chamber as the reactant. The distance between the target and sample was 20 cm, and the substrate rotation speed was 60 RPM. For the deposition of rectifying interphase on LLZTO pellets, the pellets were purchased from Limao Tech Co Ltd with a diameter of 14.1 mm and a thickness of 1mm. The pellets were polished with sandpaper (from 300 to 7000 grit) to achieve a glazed surface. The pellets were cleaned with high-pressure N_2 gas blowing and then transferred into the high vacuum chamber for sputter deposition with similar parameters as on-chip devices. Then, the layers of Al (25 nm), p-Si (10 nm) and n-TiO_2 (10 nm) were created using a sputtering power of 150 W with sputtering times of 1000 s, 500s and 600 s, respectively. Once the deposition was complete, the pellets were transferred to an Ar-filled glovebox for storage. The external Al layer needs to be thick enough to provide adequate protection for the internal junction, which is determined by the duration of air exposure. The minimum thickness required for the rectifying junction is to achieve a stable asymmetric conductance, which is influenced by materials, doping profile and interface geometry. On this basis, the thickness should be as minimal as possible to reduce any side effects on ion transport.

Structure characterisation

The structure of the as-purchased LLZTO pellets was characterised by the X-ray diffraction (PANalytical X'Pert Pro) technique (**Fig S13**), showing a cubic structure agreeing well with previous reports.[1] X-ray photoelectron spectroscopy (XPS) was acquired using a Theta probe. For the depth profiling, a 3 kV Ar^+ was used with 25 s per step for etching (total step: 250). XPS spectra were collected after each step. The time-of-flight secondary ion mass spectrometry (ToF-SIMS) data were acquired using an OrbiSIMS (HybridSIMS, IONTOF GmbH, Germany) instrument.[2] Positive ion sputter depth profiles were measured in the non-interlaced mode using a repeating sequence of ToF-SIMS analysis from a 200 μm × 200 μm field of view centred in the 300 μm × 300 μm field of view of the subsequent sputtering cycle. The analysis cycle was conducted with 30 keV Bi_3^+ primary ions with a beam current of 0.23 pA for 200 μs. A 2 keV O_2 beam was used in the sputter cycle with a beam current of 3.9 nA. Both ion beams have an angle of incidence of 45° with the sample surface are set 90° apart in the azimuthal plane. Data analysis was performed using Surfacelab 7.1 (IONTOF GmbH).

Electrochemical characterisation

The 300 nm gold deposition of ionic blocking electrodes was realised by E-beam deposition (Alliance Concept EVA-450). Electrochemical impedance spectroscopy was performed with an electrochemical workstation (Gamry

Reference 600+). Li plates (diameter of 12 mm and thickness of 0.5 mm) were used as purchased (Tob New Energy Technology Co., Ltd.). The Li symmetric cells were prepared in an Ar-filled glove box. To assemble Li symmetric cells, the Li plates and the pellet (with deposition on both sides) were used as electrodes and the electrolyte, respectively. Two Li plates were attached on each side of the pellet between two stainless steel meshes and heated to 200 °C via a hot plate. The sandwich-like structure was then mounted into a CR2032 coin cell case, and the cell was also heated to realise a conformal interface contact. The cell was cooled down to room temperature for electrochemical testing. The hybrid full cells with NMC811 cathode and Li metal anode were also assembled in the CR2032 coin cell case. The NMC811 cathode electrode was prepared via a common slurry coating process on Al foil. The electrode consisted of 70% active material, 20% carbon black, and 10% polyvinylidene fluoride (PVDF) binder. N-methyl-2-pyrrolidone (NMP) was used as the solvent for slurry preparation. 1 M $LiPF_6$ in EC/DEC [1:1 (v/v)] electrolyte was added onto the surface of the cathode electrode with the loading of 5 μL cm^{-2}. The voltage window for hybrid full cell testing was set to 3.0 – 4.2 V. The galvanostatic cycling performance was tested via a battery testing system (CT-4008-5V10mA, Neware Technology Ltd.). The cell clips were used to provide gentle pressure to ensure good continuous contact.

3D microstructural characterisation by X-ray computed tomography

The pristine/cycled LLZTO and LLZTO-RI samples were scanned using a Zeiss Xradia Versa 620 X-ray microscope (Carl Zeiss, CA, USA). A polychromatic cone-beam generated at the accelerating voltage of 120 kV was used for the target transmission ratio of approx. 0.25. 2001 projections were taken over 360° rotation, with an exposure time of 40 seconds and a spatial resolution of 0.95 μm. A proprietary Feldkamp-Davis-Kress (FDK) algorithm[3] was used for the 3D reconstruction of the SSEs, which were then imported into the commercial software package Avizo v2022 (Avizo, Thermo Fisher Scientific, Waltham, Massachusetts, U.S.) for visualisation and quantification of the porosity and pore size distribution.

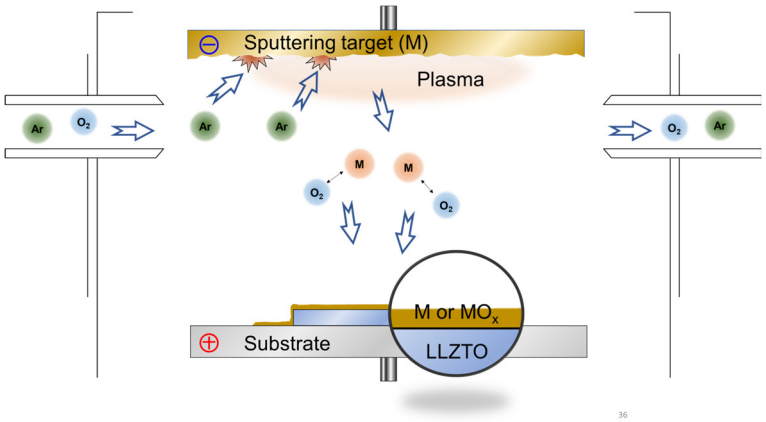

Fig S1 Schematic diagram of the direct current sputter deposition approach for the fabrication of the on-chip device and the deposition of rectifying interphase. The target materials were bombarded with ionised noble gas, resulting in the atoms being sputtered off the targets into a plasma. These vaporised atoms were then deposited and condensed as a thin film, coating the external surface of the substrate.

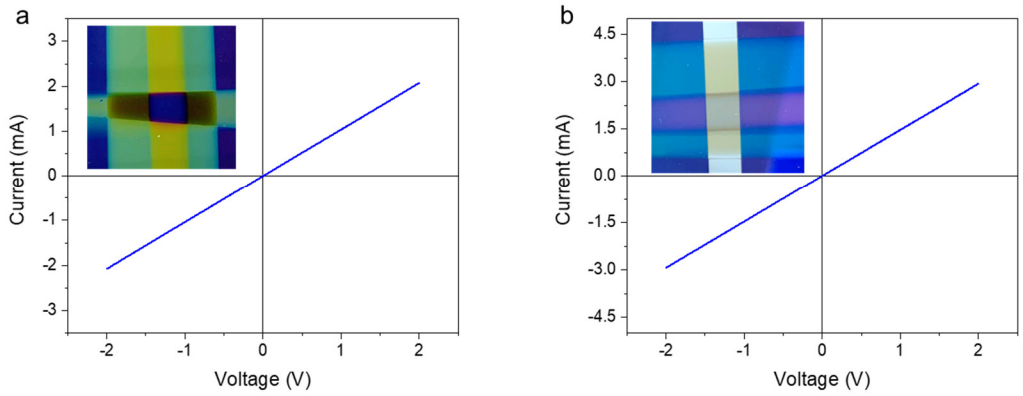

Fig S2 *I-V* characteristics of (a) Al/TiO_2/Ti and (b) Al/Si/Ti devices. Inset: digital photograph of fabricated on-chip devices.

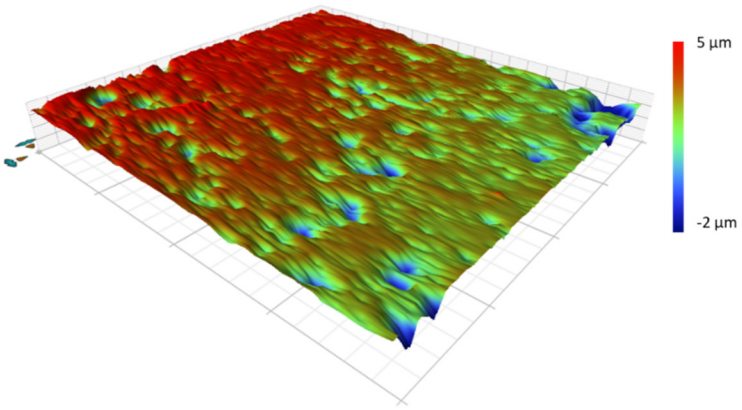

Fig S3 Surface topography mapping of LLZTO pellet using a Dektak stylus profilometer.

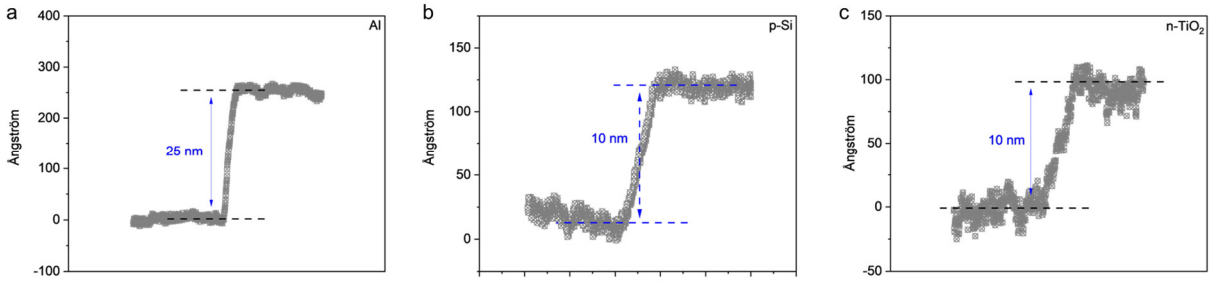

Fig S4 Thickness measurement of deposited layers on Si wafer using a Dektak stylus profilometer.

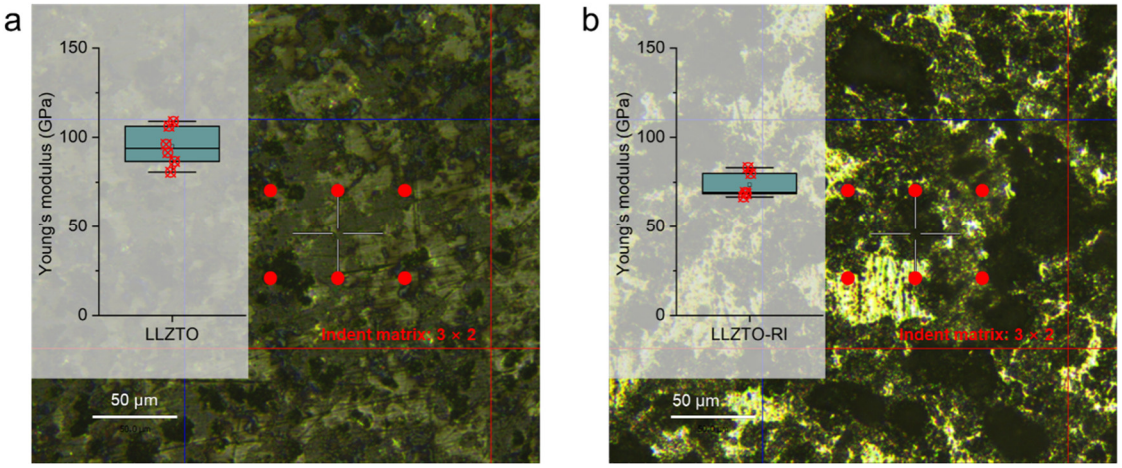

Fig S5 Optical microscope images and nanoindentation results of (a) the LLZTO sample and (b) the LLZTO-RI sample. The variation in contrast observed in the microscope image of LLZTO-RI is due to the reflection of light by the external Al layer on the surface of the LLZTO-RI sample.

Nanoindentation was performed using an Ultra Nanoindentation Tester (UNHT^3, Anton Paar, Austria), equipped with a diamond Berkovich indenter, of which the area function was calibrated with certified reference materials. Nanoindentation experiments were conducted under load-control, with a maximum load of 30 mN to achieve an indentation depth of about 650 nm, while applying and removing the load within 30 s. At the maximum load, a dwell period of 60 seconds was maintained before unloading, as well as another dwell period of 60 s at 90 % of unloading for monitoring thermal drift. A matrix of 3×2 indents were performed as shown in **Fig S5**.

The LLZTO pellet exhibited a Young's modulus of 95 ± 10 GPa with a Poisson's ratio of 0.25. The results obtained from the surface of the LLZTO-RI sample show a Young's modulus of 75 ± 5 GPa. The decrease in Young's modulus is predominantly attributed to the external Al layer, which has a theoretical modulus of < 70 GPa. On the other hand, the sputtering deposited layers can cover the surface flaws and defects, which might contribute to prevent dendrite generation from the Li metal anode side.

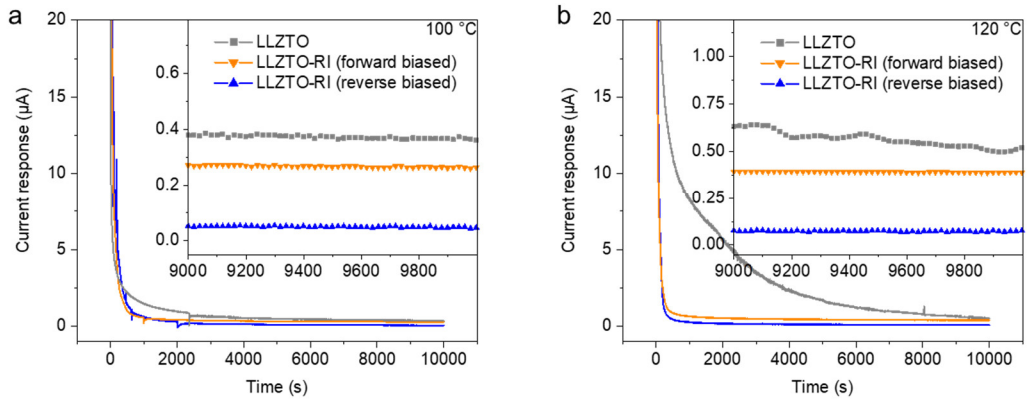

Fig S6 Chronoamperometry curves for the solid-state electrolyte pellets under a constant polarisation of 1 V at (a) 100 °C and (b) 120 °C, respectively.

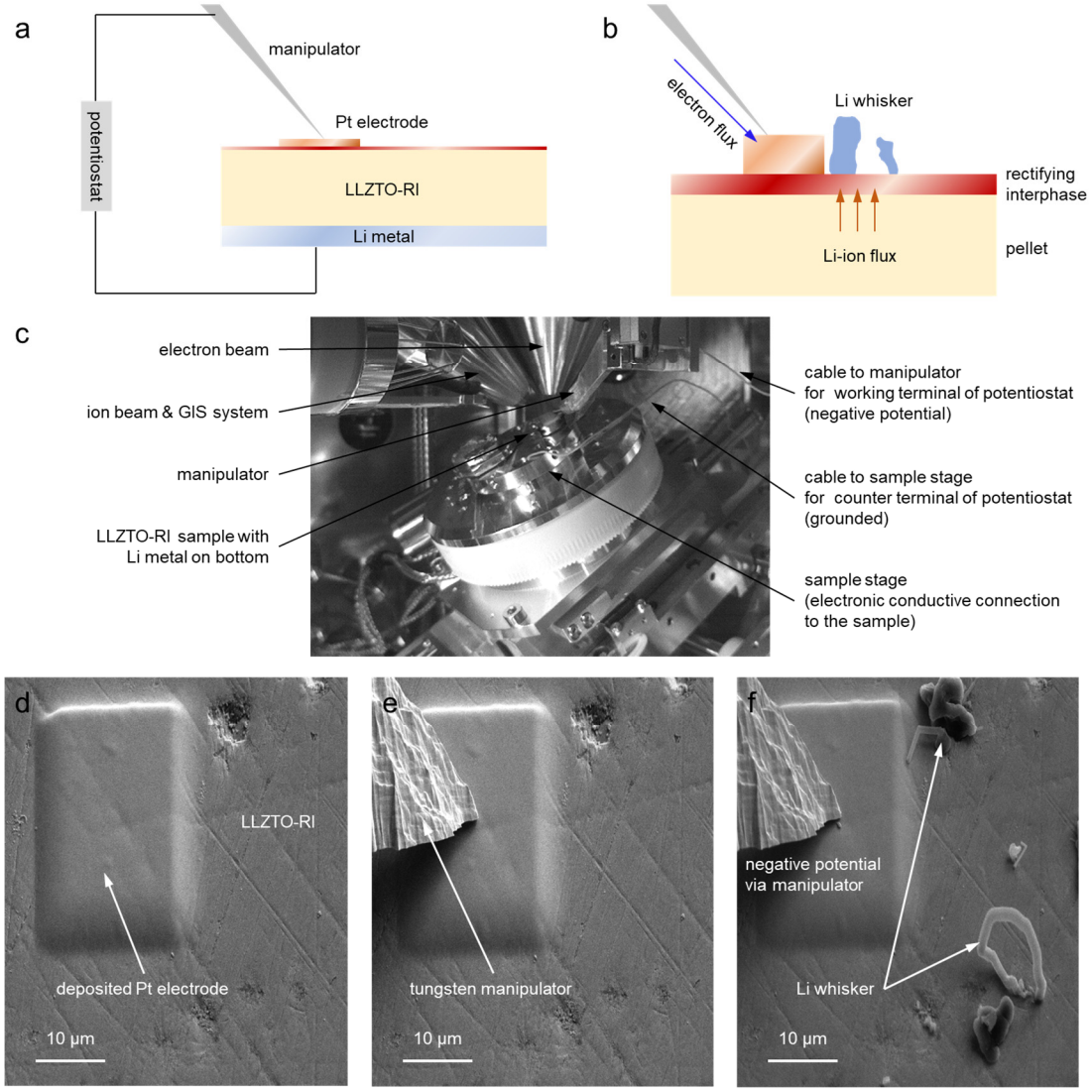

Fig S7 *In-situ* observation of Li plating on the surface of LLZTO-RI (without Al layer) via an *in-situ* SEM platform. (a-b) Schematic of the Li plating experiment on the surface of LLZTO-RI. (c) Optical photo of the SEM chamber, showing the relative position and connection of each part. (d-f) SEM images of the Li plating region.

The *in-situ* observation was conducted using a combination of the TESCAN LYRA3 FIB-SEM and the Gamry potentiostat (Reference 600+). The LLZTO-RI pellet with rectifying interphase coating on one side was placed on a Li metal chip (**Fig S7a**). Thermal treatment was performed to ensure proper contact. The Li metal was then mounted on a stub which was fixed on the stage. The stage was connected to the counter terminal of the potentiostat. The connection of each part is shown in **Fig S7c**. A small Pt pad was deposited on the surface of LLZTO-RI as a current collector through the gas injection system (GIS) (**Fig S7d**). The tungsten manipulator was connected to the working terminal of the potentiostat and brought into contact with the Pt pad (**Fig S7e**). A negative potential was applied via potentiostat. As shown in **Fig S7f**, the Li-ions was able to transport across the rectifying interphase and plate on the surface of the LLZTO-RI sample.

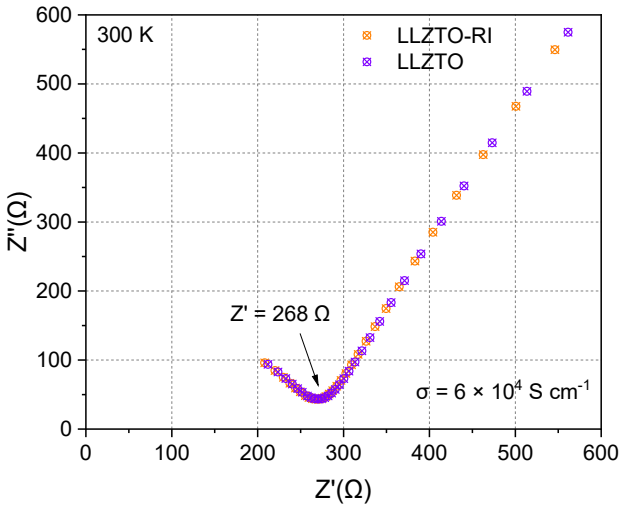

Fig S8 EIS profiles of the Au/SSE/Au cells at room temperatures, indicating similar ionic conductivity after the deposition of the rectifying interphase.

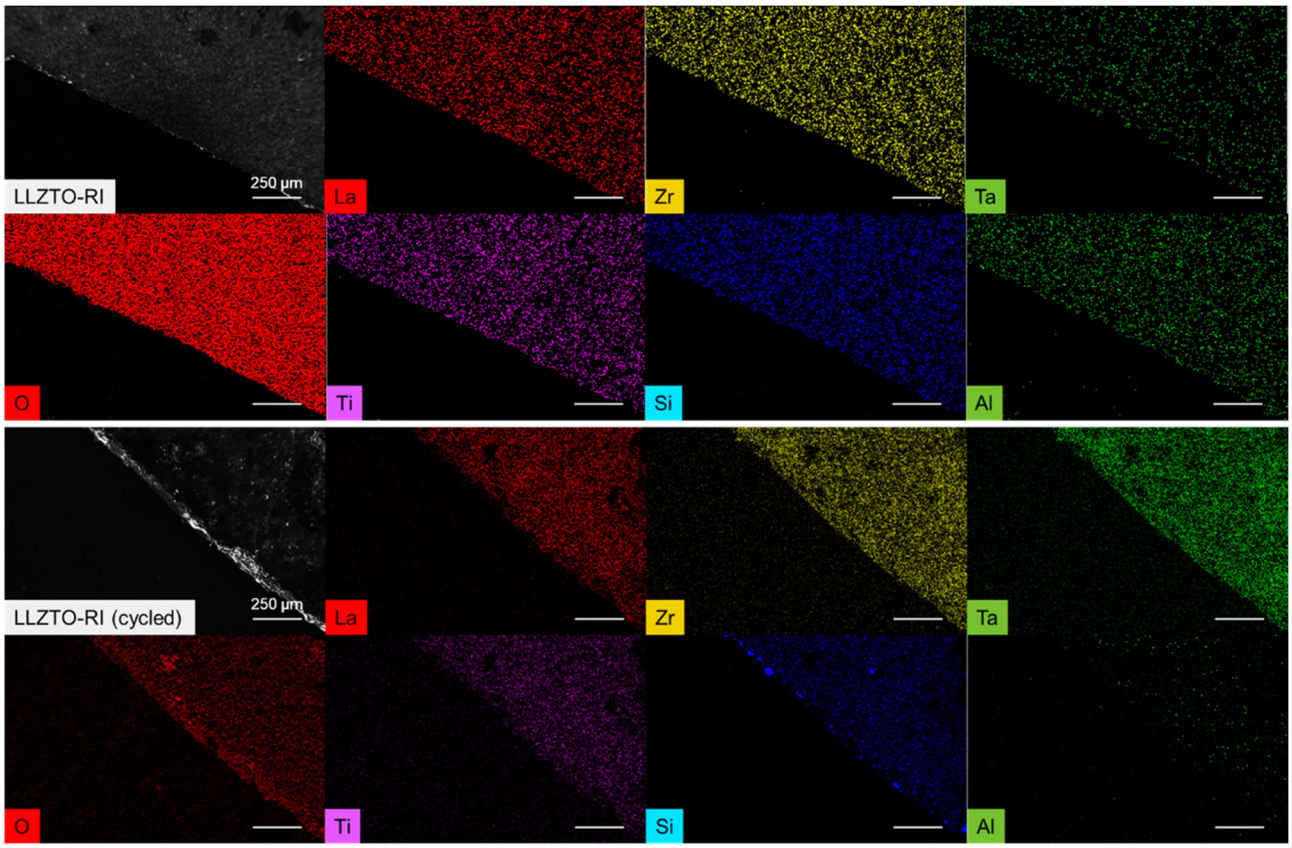

Fig S9 EDS chemical mapping of the LLZTO-RI pellets before and after electrochemical cycling. The Li metal electrodes were removed via thermal treatment. In the pristine LLZTO-RI sample, the La, Zr and Ta signals are attributed to the LLZTO, and the Ti, Si and Al signals correspond to the rectifying interphase. After cycling, the EDS chemical mappings reveal no substantial Al signal on the surface due to the spontaneous reaction between Al and Li metal, whilst the existence of Ti and Si after cycling was indicated.

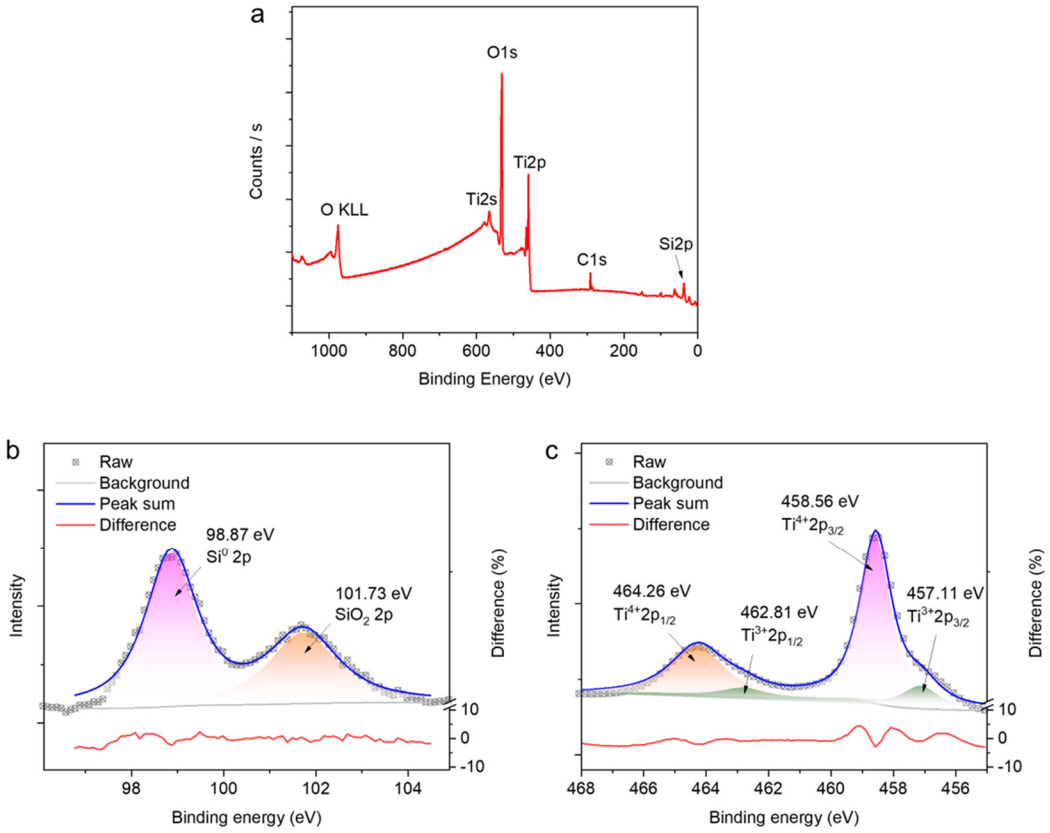

Fig S10 XPS analysis for the cycled LLZTO-RI sample. The Li metal electrodes were removed via thermal treatment. (a) XPS survey spectra of the sample indicate the existence of Si and Ti, whilst no Al signal was detected. These results agree with the EDS chemical mapping in ***Fig S9***. (b) High-resolution Si 2p core level spectrum with curve fitting shows the existence of Si, with the SiO_2 potentially resulting from the oxidation during the transfer process as there is no external Al layer to protect against ambient air. (c) High-resolution Ti 2p core level spectrum with curve fitting reveals the unsaturated coordination of Ti^{3+}, suggesting that the TiO_2 should also exhibit the n-type characteristic after cycling.

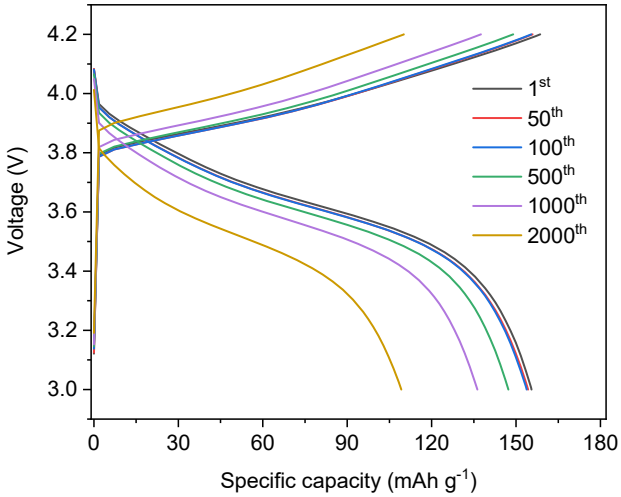

Fig S11 Voltage profiles of the hybrid full cell with NMC811 cathode at different cycles.

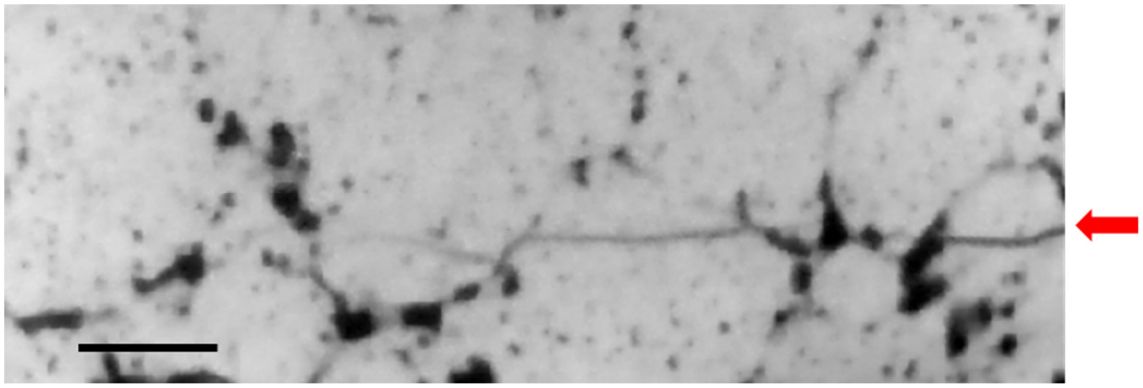

Fig S12 Zoom-in view of the transgranular cracks (red arrow) in the cycled LLZTO sample. (Scale bar: 100 μm)

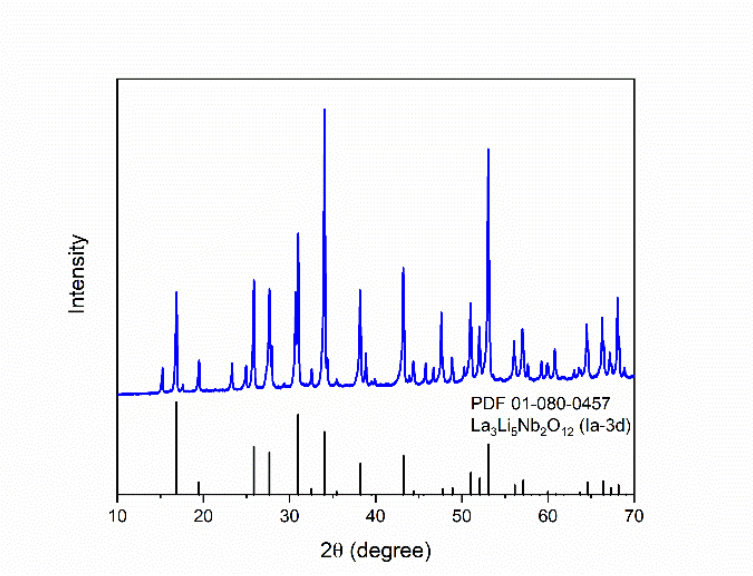

Fig S13 XRD pattern of the as-purchased LLZTO pellet.

Reference

1. Y. Ren, T. Liu, Y. Shen, Y. Lin and C.-W. Nan, *J. Materiomics*, 2016, **2**, 256-264.
2. M. K. Passarelli, A. Pirkl, R. Moellers, D. Grinfeld, F. Kollmer, R. Havelund, C. F. Newman, P. S. Marshall, H. Arlinghaus and M. R. Alexander, *Nat. Methods*, 2017, **14**, 1175-1183.
3. J. Hsieh, B. Nett, Z. Yu, K. Sauer, J.-B. Thibault and C. A. Bouman, *Current Radiology Reports*, 2013, **1**, 39-51.